Supporting information

Fast carbon dioxide–epoxide cycloaddition catalyzed by metal and metal-free ionic liquids for designing non-isocyanate polyurethanes

Marwa Rebei,[a,b] Ctirad Červinka,[c] Andrii Mahun,[a,b] Petra Ecorchard,[d] Jan Honzíček,[e] Sébastien Livi,[f] Ricardo K. Donato,[g] Hynek Beneš[a,*]

[a] *Institute of Macromolecular Chemistry of the Czech Academy of Sciences, Heyrovského nám.2, Prague 6, 162 00, Czech Republic*

[b] *Department of Physical and Macromolecular Chemistry, Faculty of Science, Charles University, Hlavova 8, 12843 Prague, Czech Republic*

[c] *Department of Physical Chemistry, University of Chemistry and Technology Prague Technická 5, CZ-166 28 Prague 6, Czech Republic*

[d] *Institute of Inorganic Chemistry of the Czech Academy of Sciences, Husinec-Řež 1001, 250 68 Řež, Czech Republic*

[e] *Institute of Chemistry and Technology of Macromolecular Materials, Faculty of Chemical Technology, University of Pardubice, Studentská 573, 532 10, Pardubice, Czech Republic*

[f] *Université de Lyon, CNRS, Université Claude Bernard Lyon 1, INSA Lyon, Université Jean Monnet, UMR 5223, Ingénierie des Matériaux Polymères, F-69621 Cédex, France*

[g] *National University of Singapore, Center for Advanced 2D Materials, Singapore 117546, Singapore*

E-mail: benesh@imc.cas.cz

Metal-based ionic liquids (MILs)

Firstly, the synthesized MILs, $(BMIM)_2ZnCl_4$ and $(BMIM)_2CoCl_4$, were characterized to prove the IL structure. The ^1H and ^{13}C NMR spectra of $(BMIM)_2ZnCl_4$ are shown in Fig. S1 and S2 and compared to BMIMCl.

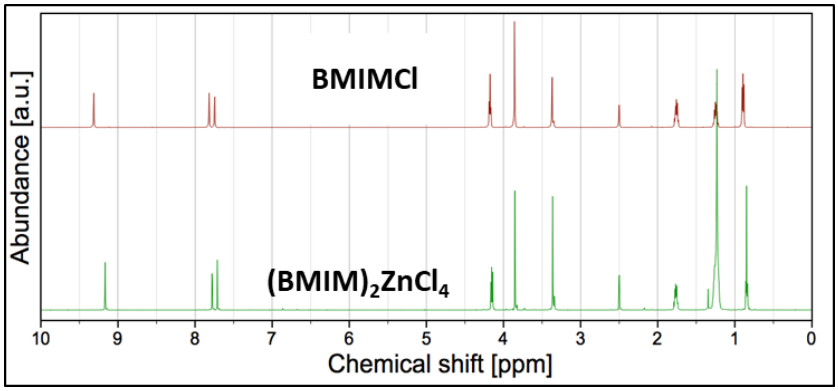

Fig. S1. ^1H NMR (DMSO-D6) of BMIMCl and $(BMIM)_2ZnCl_4$. BMIMCl: δ 0.893 (t, H_3C-) 1.247 (m, -CH_2-CH_3) 1.758 (p, -CH_2-CH_2-CH_3) 3.371 (s, H_2O) 3.856 (s, H_3C-N) 4.174 (t, -CH_2-CH_2- CH_2-CH_3) 7.746 (s, H_2C=CH_2-N-R) 7.817 (s, H_2C=CH_2-N-CH_3) 9.314 (s, N-C*H*-N). $(BMIM)_2ZnCl_4$: δ 0.848 (t, H_3C-) 1.232 (m, -CH_2-CH_3) 1.776 (p, -CH_2-CH_2-CH_3) 3.363 (s, H_2O) 3.851 (s, H_3C-N) 4.152 (t, -CH_2-CH_2- CH_2-CH_3) 7.711 (s, H_2C=CH_2-N-R) 7.779 (s, H_2C=CH_2-N-CH_3) 9.314 (s, N-C*H*-N).

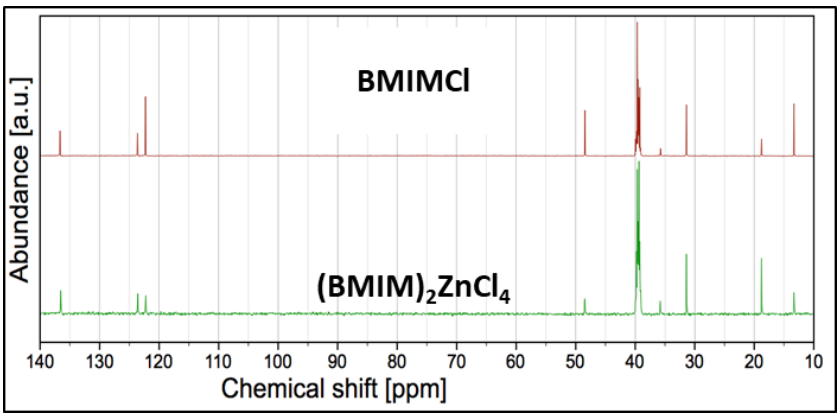

Fig. S2. ^{13}C NMR (DMSO-D6): of BMIMCl and $(BMIM)_2ZnCl_4$. BMIMCl: δ 13.321 (1C, -*C*H_3) 18.793 (1C, -*C*H_2-CH_3) 31.391 (1C, -*C*H_2- CH_2-CH_3) 35.748 (1C, H_3C-N) 48.446 (1C, *C*H_2-CH_2- CH_2-CH_3) 122.287 (1C, H_2C=*C*H_2-N-R) 123.621 (1C, H_2C=*C*H_2-N-CH_3) 136.642 (1C, N-*C*H-N). $(BMIM)_2ZnCl_4$: δ 13.321 (1C, -*C*H_3) 18.793 (1C, -*C*H_2-CH_3) 31.401 (1C, -*C*H_2-CH_2-CH_3) 35.827 (1C, H_3C-N) 48.501 (1C, *C*H_2-CH_2- CH_2-CH_3) 122.269 (1C, H_2C=*C*H_2-N-R) 123.615 (1C, H_2C=*C*H_2-N-CH_3) 136.530 (1C, N-*C*H-N).

The ^{1}H NMR spectra proved the formation of a typical imidazolium ring in $(BMIM)_2ZnCl_4$ by the presence of signals at δ =3.85 (s, H_3C-N), 7.71 (s, H_2C=CH_2-N-R), and 9.166 (s, N-C*H*-N).[1] The metal contents (%) in $(BMIM)_2ZnCl_4$ and $(BMIM)_2CoCl_4$ were calculated using elemental analysis (AAS). The results showed that the experimental metal content values Zn (11.04%) and Co (12.74%) are very close to the theoretical values, 11.03 and 12.30 %, respectively [2,3], suggesting the effective insertion of the metal centre (Zn and Co) in the imidazolium IL. When comparing FTIR spectra and thermogravimetric analyses (TGA) of BMIMCl with $(BMIM)_2CoCl_4$, and $(BMIM)_2ZnCl_4$, the MILs showed a low level of absorbed water (approximately 1 wt%) (Fig. S3).

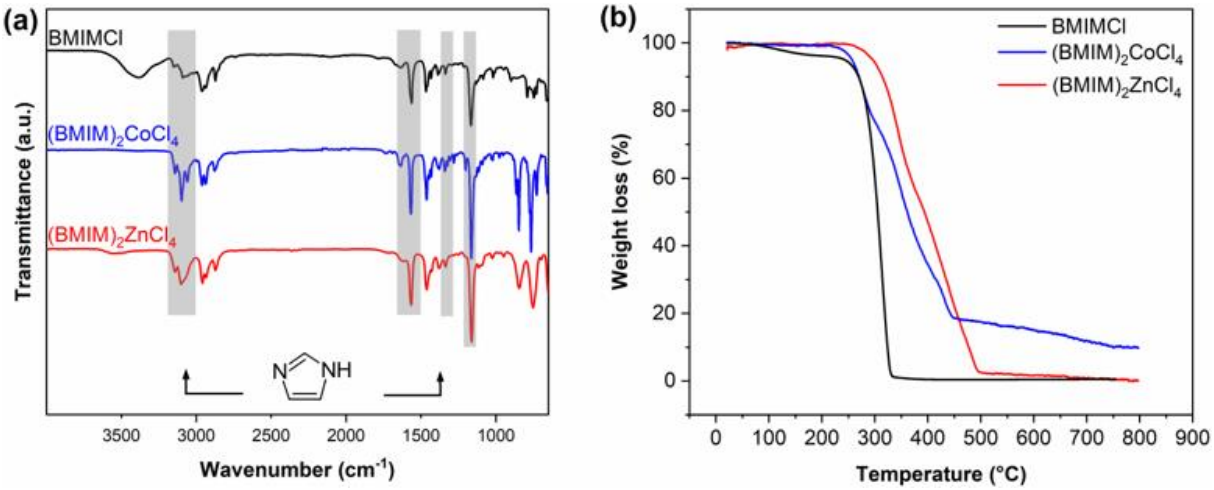

Fig. S3. (a) FTIR spectra and (b) TGA curves of BMIMCl, $(BMIM)_2CoCl_4$ and $(BMIM)_2ZnCl_4$.

FTIR spectra of $(BMIM)_2CoCl_4$, and $(BMIM)_2ZnCl_4$ exhibited typical characteristic bands from the imidazolium ring proved by the presence of bands at 3090 - 3142, 1563 - 1640, and 1163 cm^{-1}, respectively attributed to the alkyl stretching in imidazole ring (C-H), imidazole ring stretching, and bending of H-C-C and H-C-N bonds (Fig. S3a).[4,5] The formation of aliphatic (C-H) alkyl chains were also confirmed by the peaks at 2690, 2877, and 2933 cm^{-1}.[5] Thermograms of $(BMIM)_2CoCl_4$ and $(BMIM)_2ZnCl_4$ showed four decomposition steps, unlike BMIMCl which showed only two steps (Fig. S3b). This proves the presence of the inorganic material, anionic metal centre into the IL, which starts decomposing at the final stage of the TGA analysis at temperature after 430 to 547 °C. Moreover, these MILs showed to be thermally stable at *T* lower than 100 °C, as the first decomposition step starts at onset *T* of approximately 240 °C, which means that the metal salts do not decompose at the reaction temperature selected in this study (80 °C), and their catalytic activity will not be compromised. The high thermal

stability of the compound is also due to the imidazolium cation that proved to be more thermally and chemically stable than other cations of ILs, such as pyridinium, or phosphonium salts.[6] The addition of the metal anionic centre was proved to enhance the Lewis acidity of the ionic liquid, hence increasing its nucleophilic character and therefore catalytic activity.[7] These properties provided by the MILs offer the opportunity to use them as new catalytic tools for the CO_2 cycloaddition reaction.

Synthesis of cyclic carbonates

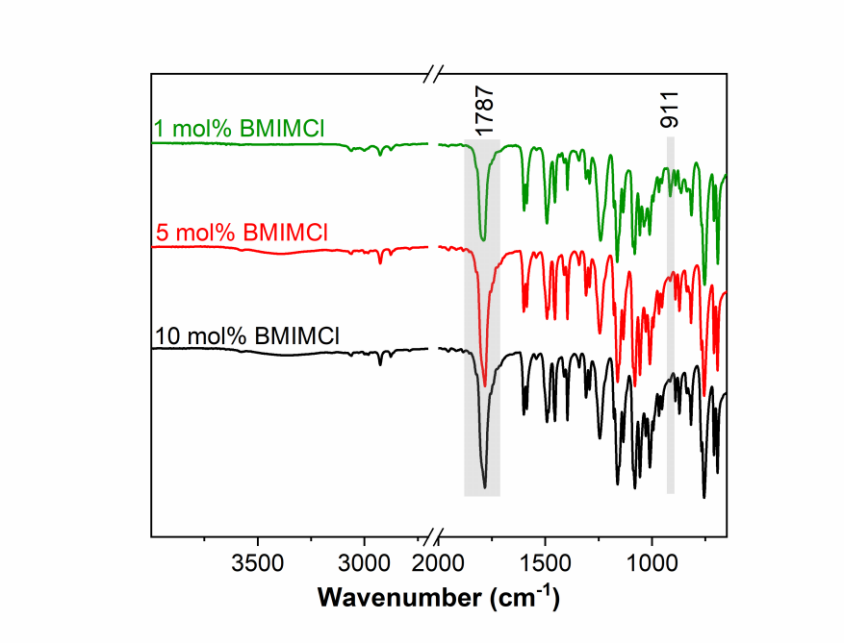

Fig. S4. FTIR spectra of PGE/CO_2/BMIMCl reaction products at different concentrations of IL (1, 5 and 10 mol%), and at reaction conditions (T=80 °C, P(CO_2)=7.7 MPa).

Computational investigation of the mechanism

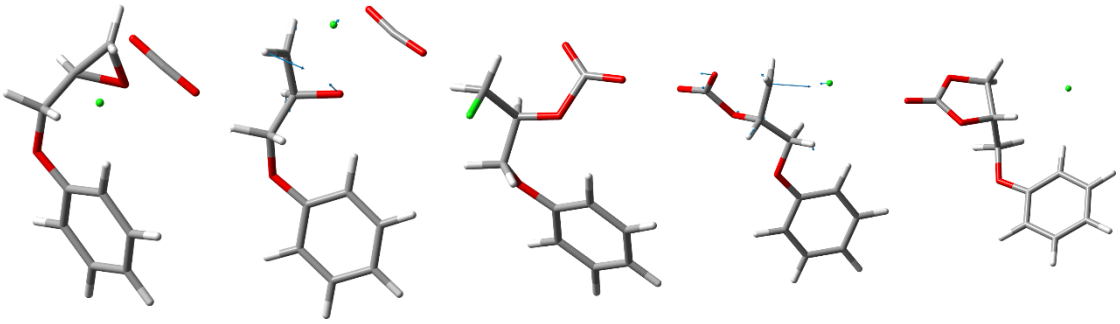

Fig. S5. Geometries of the important points along the overall reaction mechanism in the minimum representation departing from a 1:1 mixture of reactants catalyzed by a chloride anion. From left to right: reactants in an optimum mutual configuration, transition state for CO_2 fixation, chloro-carbonate intermediate, transition state for carbonate cyclisation, and cyclic carbonate product. Eigenvectors of the single internal mode exhibiting an imaginary vibrational frequency are depicted for both transition states.

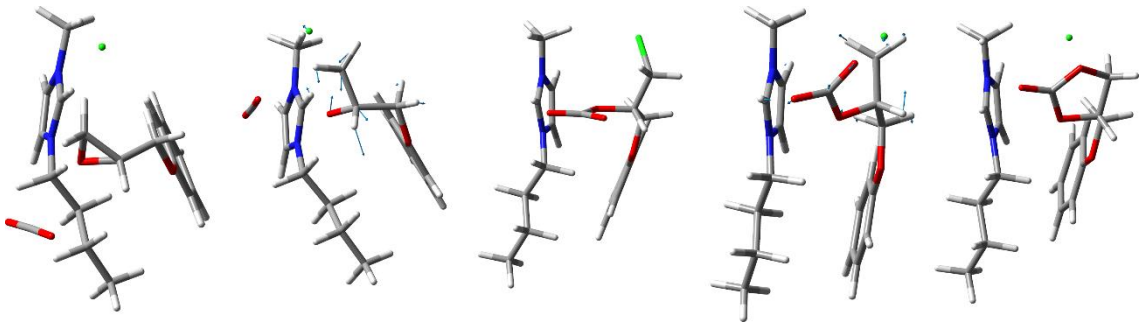

Fig. S6. Geometries of the important points along the overall reaction mechanism in the explicitly solvated representation including one whole BMIMCl ion pair in excess to the 1:1 mixture of reactants. From left to right: reactants in an optimum mutual configuration, transition state for CO_2 fixation, chloro-carbonate intermediate, transition state for carbonate cyclisation, and cyclic carbonate product. Eigenvectors of the single internal mode exhibiting an imaginary vibrational frequency are depicted for both transition states.

Table S1. Relative Gibbs energies (at 298 K, in kJ mol^{-1}) of important entities along the reaction of PGE with CO_2 in BMIMCl, as obtained from B3LYP-D3(BJ)/6-311+G(d,p) level of theory and for various solvation models of implicit (PCM), explicit (including 1 or 2 ionic pairs), and full (combining implicit and explicit) solvation. Explicit solvent particles are noted in brackets.

Solvation model	REAC	TS1	INT	TS2	PROD	BAR1	BAR2
Vacuum (1 Cl^-)	66.0	244.8	60.1	110.0	0.0	178.8	49.9
PCM (1 Cl^-)	50.1	245.7	49.1	118.2	0.0	195.6	69.1
Vacuum (1 $BMIM^+$ & 1 Cl^-)	33.4	198.5	31.6	128.4	0.0	165.2	96.8
PCM (1 $BMIM^+$ & 1 Cl^-)	40.9	226.7	43.0	118.9	0.0	185.9	76.0
Vacuum (2 $BMIM^+$ & 2 Cl^-)	29.9	104.6	32.5	114.1	0.0	74.7	81.5
PCM (2 $BMIM^+$ & 2 Cl^-)	40.5	139.5	40.9	128.1	0.0	99.0	87.2

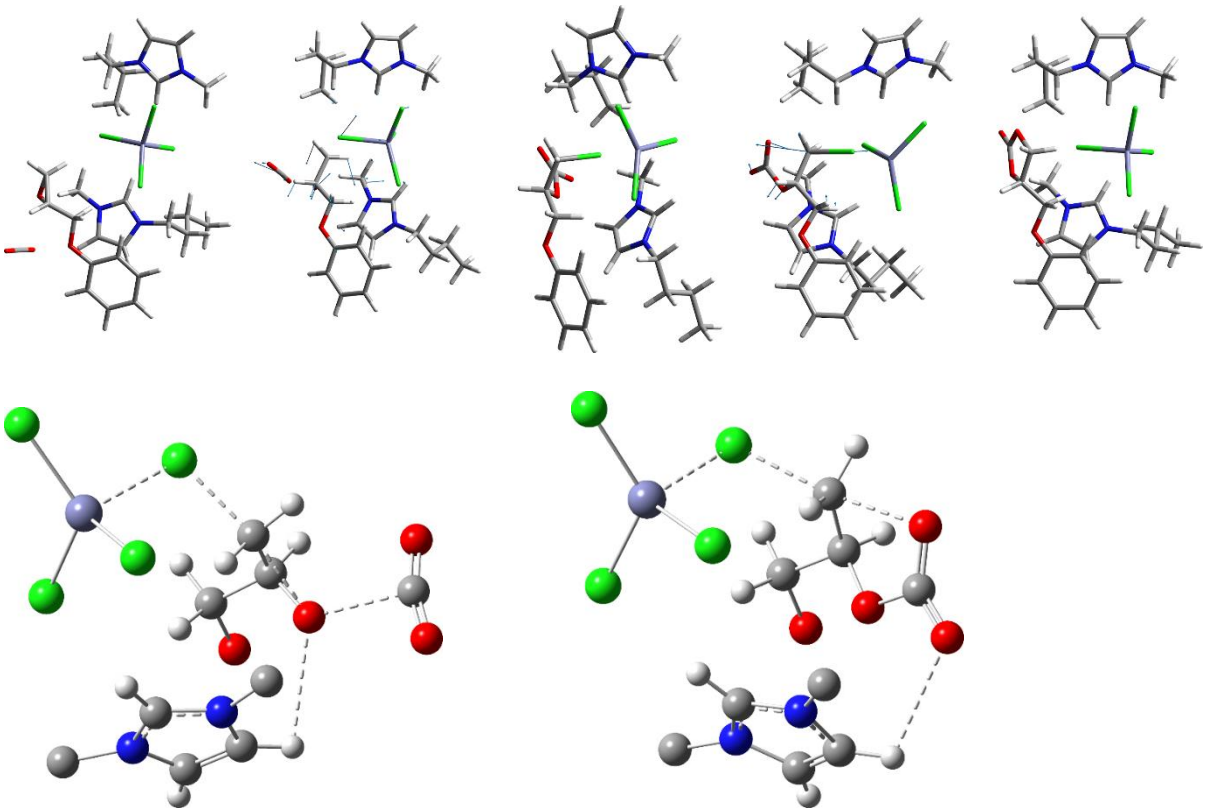

Fig. S7. Geometries of the important points along the overall reaction mechanism in the explicitly solvated representation including one explicit $(BMIM)_2ZnCl_4$ entity in excess of the 1:1 mixture of reactants. First row, from left to right: reactants in an optimum mutual configuration, transition state for CO_2 fixation, chloro-carbonate intermediate, transition state for carbonate cyclisation, and cyclic carbonate product. Eigenvectors of the single internal mode exhibiting an imaginary vibrational frequency are depicted for both transition states. Second row: a detailed view of the most important fragments of the reacting species representing TS1 and TS2 clusters.

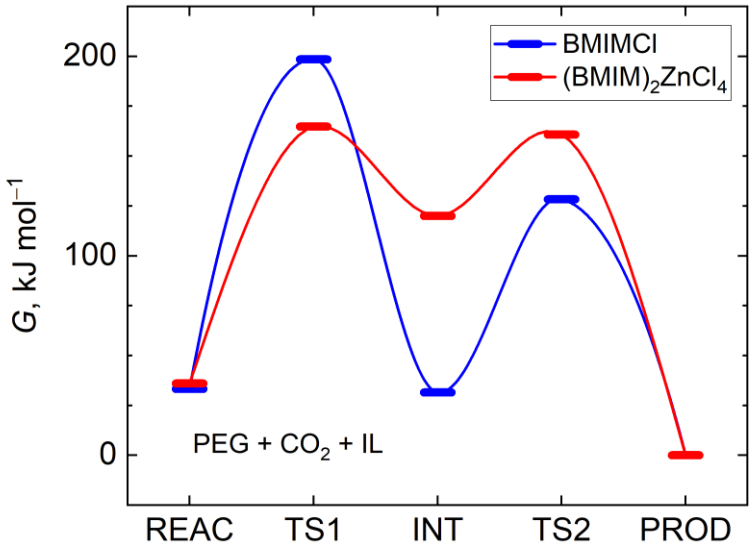

Fig. S8. Gibbs energy profiles along the suggested reaction paths as modelled at the B3LYP-D3/6-311+G(d,p) level of theory. Energies of the reactants, intermediate entities, products, and transition states are compared for the reactions occurring in a vacuum in the explicit presence of a single stoichiometric entity of BMIMCl or $(BMIM)_2ZnCl_4$. Lines interconnecting individual states are only for guide-the-eye.

References

1 H. S. Kim, J. J. Kim, H. Kim and H. G. Jang, *J. Catal.*, 2003, **220**, 44–46.

2 J. Palgunadi, O. S. Kwon, H. Lee, J. Y. Bae, B. S. Ahn, N. Y. Min and H. S. Kim, *Catal. Today*, 2004, **98**, 511–514.

3 C. Zhong, T. Sasaki, A. Jimbo-Kobayeshi, E. Fujiwara, A. Kobayashi, M. Tada and Y. Iwasawa, *Bull. Chem. Soc. Jpn.*, 2007, **80**, 2365–2374.

4 D. Liu, G. Li and H. Liu, *Appl. Surf. Sci.*, 2018, **428**, 218–225.

5 T. Rajkumar and G. Ranga Rao, *Mater. Chem. Phys.*, 2008, **112**, 853–857.

6 P. Migowski, P. Lozano and J. Dupont, *Green Chem.*, 2023, 1237–1260.

7 J. Estager, J. D. Holbrey and M. Swadźba-Kwaśny, *Chem. Soc. Rev.*, 2014, **43**, 847–886.